INSTITUTE OF PHYSICS PUBLISHING JOURNAL OF PHYSICS D: APPLIED PHYSICS

J. Phys. D: Appl. Phys. **35** (2002) 3145–3152 PII: S0022-3727(02)36207-7

LISA simulations of time-reversed acoustic and elastic wave experiments

P P Delsanto[1], P A Johnson[2], M Scalerandi[1] and J A TenCate[2]

[1] INFM, Dip. Fisica, Politecnico di Torino, C.so Duca degli Abruzzi 24, 10129, Torino, Italy
[2] Los Alamos National Laboratory, Geophysics Group, MS D-443, Los Alamos, NM 87545, USA

Received 25 April 2002
Published 18 November 2002
Online at stacks.iop.org/JPhysD/35/3145

Abstract
Several experiments in the last decade have demonstrated the enormous potential of time-reversed acoustic (TRA) and elastic (TRE) waves for applications in many fields, such as medicine, materials characterization and oceanography. In the present contribution, we demonstrate the applicability of the local interaction simulation approach (LISA) to simulate, by means of virtual experiments, both TRA and TRE and to reproduce the relevant features of both techniques.

1. Introduction

The basic solutions to the one-dimensional linear wave propagation equation for electromagnetic, acoustic or ultrasonic waves are well known: $f(x - vt)$ and $g(x + vt)$. These solutions are usually interpreted as describing pulses travelling forwards and backwards, respectively, with respect to the positive direction of the x-axis. An equally legitimate interpretation is that of pulses travelling forwards and backwards in time (time invariance). In the acoustic case, this alternative interpretation implies that, for every burst of sound $u_S(r, t)$ propagating away from a source in any reflecting, refracting or scattering medium, there exists a set of pulses $u_R(r, -t)$, which precisely retrace all the paths generated by the propagation of u_S arriving simultaneously at the sound source.

Time invariance (and its violation in weak nuclear interactions) is a concept of fundamental relevance in elementary particle physics. In principle, it could be exploited in micro- and macromechanics experiments, but the extreme sensitivity to initial conditions makes it unworkable in most situations. Waves, however, are much less sensitive to initial conditions than particles. In fact, in a multiple scattering environment, the critical length that causes a significant deviation at a future time t decreases exponentially with time in the case of particles, but only as the square root of time for waves [1].

Time-reversal invariance has been used for many years by seismologists in the petroleum exploration community. However, while their method, called time-reversed migration [2–4], requires the time-reversal process to be performed by computers, with time-reversed acoustic (TRA) or time-reversed elastic (TRE) the time-reversal is accomplished in the propagation media itself.

The basic premise of both time-reversed migration and TRA is that, if the wavefield can be known as a function of time on some boundary surrounding a given region, then it can also be found at every point inside that region at previous times by using the wave equation with time running backwards. In other words, the result of a time-reversal process is that the waves recorded on the boundary are focused back on the acoustic sources or scattering targets (acting as sources) inside.

Furthermore, if recorded wavefields from an array of receivers are electronically time-reversed and transmitted back into the medium, the wavefield is focused back onto the scatterers and sent back to the receivers. The new wavefield observed at the array, however, will now be proportionally dominated by the scattering from the strongest scatterers. This effect may be further enhanced by successive iterations or by applying the so-called Décomposition de l'Operateur de Retournment Temporel (DORT) method [5, 6]. A remarkable feature of DORT is that the focusing may also be selectively implemented on weaker scatterers. In fact, it is possible to build an $N \times N$ matrix (N is the number of transmittters/receivers), whose element (i, j) is given by the signal received by the receiver j from the signal from transducer i. After time-reversal, each eigenvector of the matrix gives a signal which focuses on a different scatterer [6].

Another important advantage of TRA is that it works well in heterogenous media (actually better than in homogeneous ones). Due to the backpropagation discussed above no knowledge of medium properties is required (i.e. deviations of

the ultrasonic rays from their path due to inhomogeneities in the specimen are automatically retraced back with the correct angles, so that no correction is needed).

Finally, the application of time-reversal to acoustics and to ultrasonics seems to represent one of those extremely rare cases in which some kind of 'reversed Murphy's law' seems to apply, i.e. 'Whatever can go right, it will' in fact, as noted above, not only are waves very robust but the acoustic (or elastic) wave propagation velocity seems to be just 'right' as well. For example, the propagation velocity is sufficiently low so that in medical applications there is no interference from the patient's breathing or heartbeat (i.e. the wave frequency is sufficiently high to avoid interference from an external noise on a human timescale). However, the propagation velocity is also not so small that pulses cannot be adequately recorded and digitally inverted (which would require electronic devices working at very high frequencies). Moreover, multiple scattering in transmission experiments [7, 8] or multiple reflections in waveguides [9], instead of being a hindrance, actually improve the focusing, to below the diffraction limit of about half of a wavelength. For these reasons TRA and TRE have generated considerable excitement, both as areas of basic research and for their potential for providing detailed information about the acoustic or elastic properties of the specimen or propagation medium of interest.

Several excellent review articles have been written on the topic of TRA and time-reversal mirrors; (1) applications of TRA to experiments in shallow water or in the ocean [10–13], (2) TRA applications for the human body [14–16] and (3) applications to damaged materials for NDE purposes [17, 18]. However, to our knowledge, these techniques have not yet been applied to the Earth, nor have numerical simulations of TRE been performed. The following paper is devoted to both subjects and results of several virtual TRA and TRE experiments are presented to demonstrate their feasibility and usefulness.

2. Numerical simulations of TRE

Virtual experiments are extremely useful, not to replace actual experiments, but to confirm the soundness of the underlying ideas and to optimize the choice of parameters. In the case of TRE waves there is an additional motivation, i.e. the possibility of studying the issue of which of the three components (compressional P, and shear SH and SV) to broadcast in the beginning and to retain to retransmit in successive time-reversal iterations. In fact, in addition to time-reversal invariance, which is satisfied in adiabatic processes, TRA and TRE require spatial reciprocity. The latter is satisfied if interchanging the position of source and receiver does not alter the resulting field. This is clearly not always the case. For example, if a fluid phase is included in the propagation medium, a P-wave from a solid enters a fluid as a P-wave only, while in the reverse process an S-wave may be generated by mode conversion at the interface.

As mentioned in the introduction, applications of TRE to Earth studies could be useful, e.g.

(i) to characterize the distribution of scatterers within the Earth or portions of it. For this purpose we recall that DORT allows one to focus selectively on relatively weaker scatterers;

(ii) to better understand the geometry of magmatic intrusions and eruptions in a volcanic region, and also to characterize fault zones;

(iii) to learn more about the heterogeneity of petroleum reservoirs from seismic data.

2.1. The local interaction simulation approach

In order to solve the elastodynamic equation to simulate the propagation of ultrasonic pulses in heterogeneous materials, as a first step for TRE, we adopt the 'local interaction simulation approach' (LISA) [19, 20]. The use of LISA is particularly convenient in conjunction with parallel processing. In fact, by placing the processors into a one-to-one correspondence with the 'cells' of the discretized specimen, one can assume that each cell may have different physical properties, since the corresponding processors are mutually independent. Of course, parallel computers do not have enough processors (yet) to establish a real one-to-one correspondence. However, by using 'virtual processors' and/or by assigning different portions of the specimen to different 'real' processors, optimal efficiency in the parallelization may be easily obtained. In fact, the updating is synchronous and the iteration law is uniform, i.e. all the sites update their state at the same time and according to the same law. As a consequence, any heterogeneous system can be treated with the same ease and computer time as a homogeneous one.

An important feature of LISA is, as its name implies, the possibility of implementing at the local level very complex mechanisms, which would be extremely hard to include in an analytical treatment (e.g. in a partial differential equation). In fact, the method allows one full freedom in the choice of interactions between the nodes, which represent the material cells. It is possible, by splitting the nodes at the interfaces between contiguous material components, to include mesoscopic features and microdamages [21]. The reliability of the LISA formalism has been verified by means of many comparisons with both analytical [19] and experimental results [22].

In the LISA approach, the specimen is discretized in a two-dimensional [21] or three-dimensional grid [23]. As already mentioned, each grid point is split into subnodes (4 in two-dimensional and 8 in three-dimensional, respectively). Subnodes belonging to nearest neighbour nodes are connected by properly defined tensorial springs. Also, internal forces are defined to keep together the four subnodes belonging to the same node. Different interactions may be introduced between the subnodes (starting e.g. from continuity relations), thus simulating perfect or faulty contact or bonding [21] and/or nonclassical nonlinear effects [24]. The elastic properties of the resulting system of springs (and forces) provide the ability to describe the propagation of a disturbance along the specimen.

2.2. The procedure

The procedure adopted is straightforward. One transducer and several receivers (used as transmitters in the TR propagation) are located at selected nodes of the discretized specimen. Unless otherwise specified, we assume that the transducers dimensions are small compared to the wavelength, so that

they may be modelled as point sources. A signal is injected in the form of a forced displacement of the corresponding node, being $u^{\text{forw}}(t)$ the temporal signal. The signal $u_j^{\text{recv}}(t)$ $(j = 1, \ldots, N)$ is then received by the N receivers. A time window $(t_0 < t < t_1)$ of the signal is amplified, time-reversed, and rebroadcasted back from all receivers simultaneously. The time is reset to 0 at the end of the injection of the TR signal, which, therefore, is given by:

$$u_j^{\text{tr}}(t - t_1) = A u_j^{\text{recv}}(t_1 + t_0 - t) \qquad t_0 < t < t_1 \quad (1)$$

where A is a constant amplification factor for all the receivers.

Albeit we are dealing with linear problems, the amplification is a relevant process for the interpretation of results. Indeed, since in the forward propagation the energy of the signal injected from the transducer is spread geometrically over the whole specimen, $u_j^{\text{recv}}(t)$ is generally a low amplitude signal (eventually even smaller due to attenuation). Therefore, amplification has to be introduced in order to obtain significant focusing.

In order to have the same energy in the injection and in the TR iterations, the amplification factor has to be calculated keeping into account the number of receivers and the width of the time window. For the present purposes, we define A, so that the maximum injected displacement is the same in the forward and TR process:

$$\max_{j,t}\left(u_j^{\text{tr}}(t)\right) = \max_{t}(u^{\text{forw}}(t)) \quad (2)$$

As a consequence, the focused signal may have a larger amplitude than the injected one (particularly when a large number of receivers is used).

3. Results and discussion

In order to demonstrate the applicability of LISA to the simulation of TRA and TRE experiments, a large number of simulations were performed. We report in the following the results of a few of them.

3.1. Waveguide simulations, TRA

Starting with virtual experiments with waveguides similar to the ones performed by Fink and co-workers [8], we first show (figure 1) the basic set-up with one source on the left-hand side and an array of 13 equally spaced receivers on the right-hand side. For the simulation, we used a discretization lattice of 1500×50 space steps ($\varepsilon = 1$ mm), with a time discretization step $\tau = 0.45\,\mu$s and frequency $\omega = 0.4$ MHz. (Note that receivers and transducers are not located on the boundaries of the specimen. The specimen extends for an additional 380 mm on each side to avoid reflections from the boundaries).

Figure 2 shows a snapshot of the displacement amplitude after time-reversal of the input signal from all 13 receivers, including up to 6 'echoes' from the waveguide walls. (The nth echo is the component of the signal as received after n reflections from the waveguide walls.) In the figure, lighter tones denote larger amplitudes. (To avoid visual effects due to the choice of the amplification factor, here and in the following, the grey scales are normalized to the maximum value in the time sequence.) Good focusing can be observed on the source location with minimal energy dispersion elsewhere.

A greyscale (or colour) map of amplitudes, such as shown in figure 2, may be very useful for illustrating the overall features of the results. However, time series plots, as shown in figure 3, allow one to perform a more detailed analysis. The first plot in figure 3 displays the injected signal, a Gaussian modulated sine wave, typical of the type of actual signals injected from a piezoelectric source into a solid. The other three plots show the x-component of the displacement (in arbitrary units) vs time in the three cases of:

(i) a signal as received after time-reversal from the 13 receivers, including 6 echoes (as in figure 2);

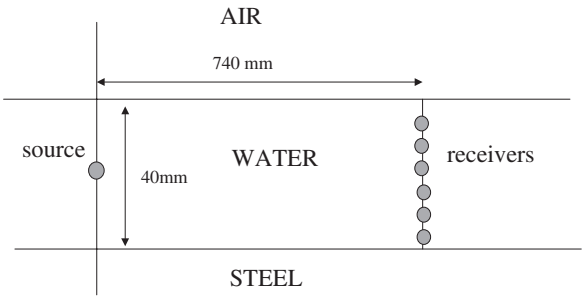

Figure 1. Set-up for the TRA virtual experiment.

Figure 2. Result of a TRA experiment using the set-up of figure 1. The grey scales are normalized to the maximum value in the considered time sequence; aspect ratio 1 : 10.

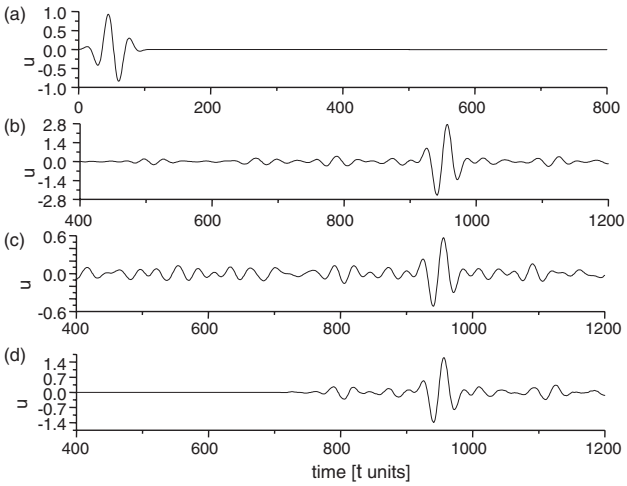

Figure 3. x-component (u) of the displacement vs time as recorded at the source location: (*a*) imput signal; (*b*) signal obtained by TRA from the 13 receivers including 6 echoes; (*c*) TRA from one receiver; (*d*) TRA from 13 receivers but using only 3 echoes. Note the different u scale in the various plots. The different amplitudes are due to a non normalized injected energy.

(ii) a signal as received after time-reversal from only one receiver (the central one);
(iii) a signal as received after time-reversal from the 13 receivers but with only 3 echoes.

It is clear from the three plots that the best focusing is obtained in the first case, as expected from previous work [7]. Case (ii) has a large level of 'noise': in fact it would be unrealistic to expect that time-reversal could be effectively carried out with a single receiver. The last plot (d), corresponding to case (iii) is much better than (c) but less focused than (b), since fewer echoes were retained, thus demonstrating the improvement power of multiple reflections, as discussed in the introduction. Note that the amplitudes of the time-reversed signals (figures 3(*b*)–(*d*)) depend on the amplification procedure adopted (see previous section). As expected from equation (1), the detected, time-reversed amplitude is larger than that of the input signal when a large number of receivers is used (figures 3(*b*) and (*d*)), and is smaller in the case of a shorter time window (figure 3(*d*)). When a single transducer is used (figure 3(*c*)) the signal is slightly smaller than the input signal in our procedure.

We next present some results of virtual TRA experiments with a pure Gaussian pulse. In figure 4, we show three successive snapshots of the displacement amplitude of the time-reversed, backward-travelling wavefield. In this case, we have considered time-reversal from all the 13 receivers and up to 9 echoes. The bottom plot again shows good focusing on the source. Figure 5 displays the component of the

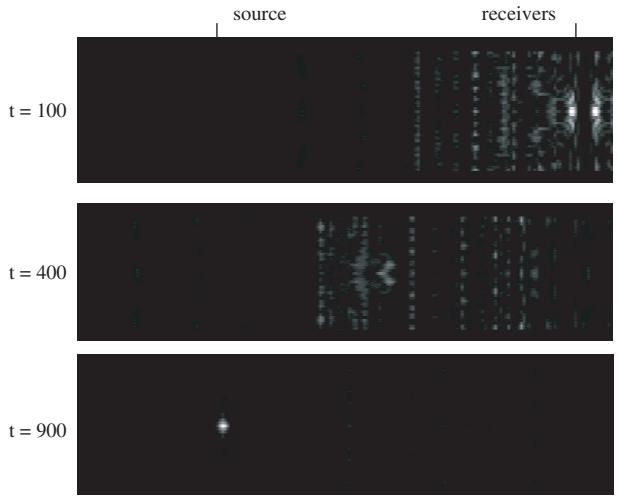

Figure 4. Snapshots of the displacement amplitude of the TR backward travelling pulse. Normalization as in figure 2.

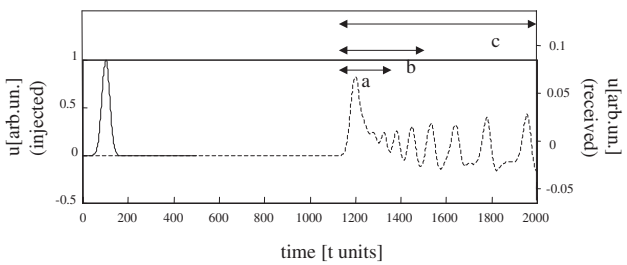

Figure 5. Injected pulse (——) and TRA signals (a,b,c) for 3, 5 and 9 echoes, respectively (- - - -).

injected pulse on the left-hand side, as recorded by the central receiver, and, on the right-hand side, the signal received by the central receiver. Note the low amplitude of the received signal (reported on the right axes) and the time windows $t_0 - t_1$ (schematically represented by the arrows a, b, c) in the cases of 3, 5 and 9 echoes, respectively, used in the reversal. Figure 6(a) shows the injected signal, (b) the 'full' time-reversed signal (13 receivers, 9 echoes), (c) the time-reversed signal from 1 receiver and 9 echoes and (d) the time-reversed signal from the 13 receivers with only 3 echoes. Again, the best result is the one obtained using the most sidewall echoes shown in figure 6(b) (same considerations on amplitudes as for figure 3).

3.2. TRE simulations

Turning our attention now to virtual TRE experiments, we consider a set-up similar to the one shown in figure 1, but with a high density solid (e.g. steel) in the waveguide and air in the bottom and top layers. The time step τ is chosen, as usual, to insure stability of the numerical procedure ($\tau = 0.15\,\mu$s). Consequently, it is smaller than in the case of water (figures 1–6), due to the higher sound velocity. Figure 7 shows snapshots at various times of the displacement amplitudes (using a Gaussian-shaped sinusoid). In the first three cases (left column) we observe the forward propagation, with the formation of Lamb-like wave patterns. In the next three plots (right column), the TR backscattered wavefield is reported, displaying good focusing on the source location in the bottom plot.

Next (figure 8), we simulate a large square solid plate (Al) with an extended source on the left-hand side and 11 equally spaced receivers on the right-hand side. The discretization lattice includes 400×400 nodes with space step $\varepsilon = 1\,$mm and a time step $\tau = 0.42\,\mu$s. The injected signal is a forward travelling Gaussian modulated sine wave with frequency $\omega = 0.5\,$MHz. As in figure 7, we show six (amplitude normalized) snapshots, the first three (left column) showing forward propagation, the last three (right column) the TR backwards travelling wavefield. Time for the

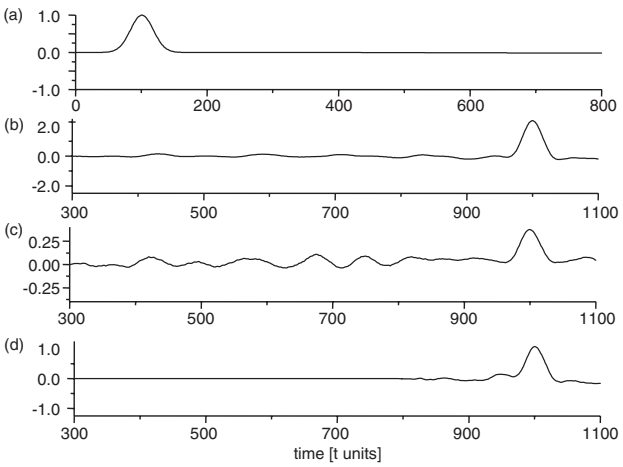

Figure 6. Time signal for the experiment of figure 4: (a) the injected pulse; (b) TRA from 13 receivers and with 9 echoes; (c) TRA from one receiver and 9 echoes; (d) TRA from 13 receivers and 3 echoes. Note the different u scale in the various plots. The different amplitudes are due to a non normalized injected energy.

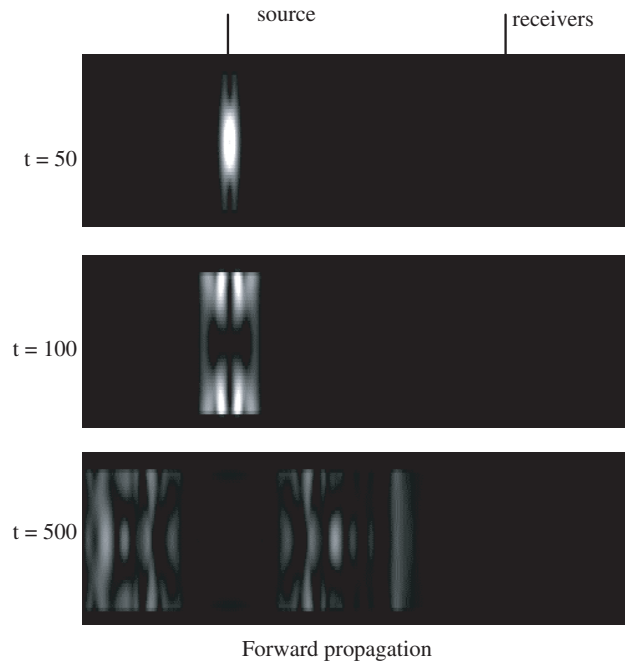

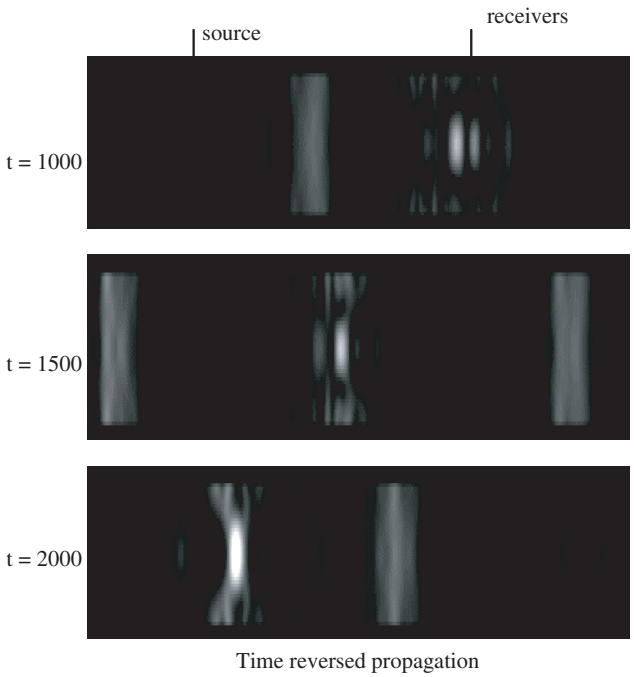

Figure 7. Forwards and time-reversed propagation of a Gaussian modulated sine wave in a steel waveguide. Normalization as in figure 2; aspect ratio 1 : 10.

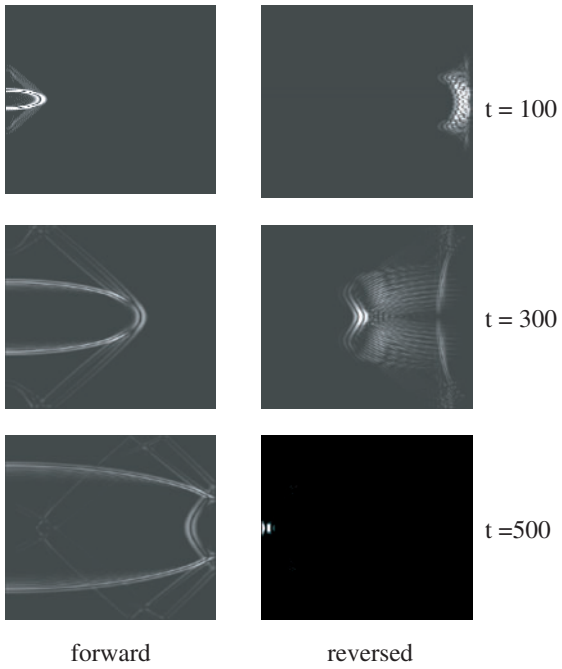

Figure 8. Forwards and backwards propagation of a Gaussian modulated sine wave in an Al plate. Normalization as in figure 2; aspect ratio 1 : 1.

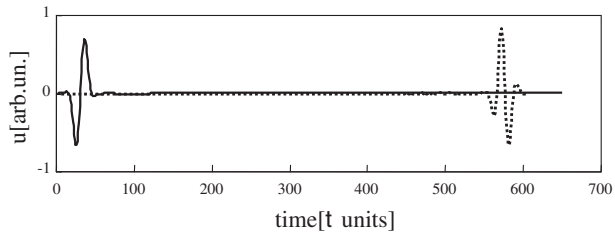

Figure 9. Injected (——) and TRE (- - - -) signals (same as in figure 8). Both signals are normalized to one.

waveforms in the right column begins from the start of the TRE procedure. In the forward propagation phase we observe the partial mode conversion to shear waves (the lateral 'wings') and reconversion to P-wave (second wavefront). The partial reflection (visible in the bottom plot) is irrelevant, since only first arrival times and amplitudes are recorded by the receivers and the broadcasting of the time-reversed signal takes place much later. In the time-reversed wavefield, it is interesting to observe the various 'rays' for the individual receivers and their convergence on the source location. Figure 9 displays the x-component of the displacement of both the injected and the TRE pulses. The absolute magnitude is not relevant here since both signals are normalized to unity. What *is* remarkable is the minimal amount of 'noise' in the TRE signal.

In order to better understand the effect of mode conversion in TRE, as discussed in section 2, we analyse four various possibilities in figure 10 (all signals have been scaled so that the x-component of the received signal is normalized to 1). The u and v components of the displacement are shown in two columns. In the upper row, the input Gaussian modulated sine wave is displayed for reference. Since it is injected as a forward travelling P-wave, it has only an x-component u (figure 10(a)); the y-component of the displacement (figure 10(b)) $v = 0$. In the second row, we display the TRE wavefield, as recorded at the source location, when the *complete* signal (i.e. both the longitudinal P and shear S) is recorded by all receivers and time-reversed (figures 10(c), (d)). In the third row the full signal is recorded, but only the x-component is time-reversed and retransmitted. Finally, in the bottom row, only the arrival of the P-wave is recorded, but *both* the x- and y-components of the displacement are rebroadcast after the time-reversal (figures 10(g) and (h)). Of these procedures, the one in the second case (figures 10(e) and (f)) yields the worst results.

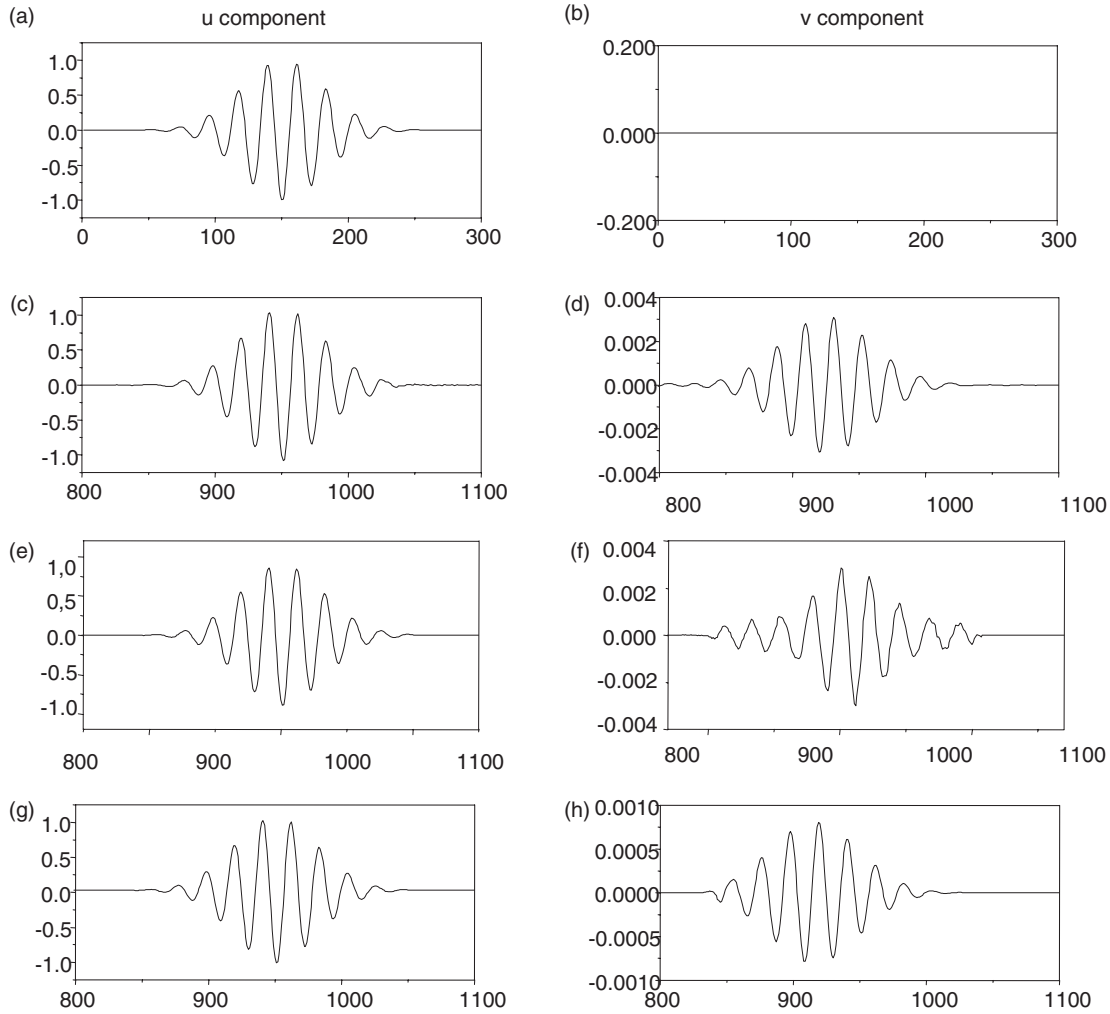

Figure 10. u and v components in the case of figure 8. First row (*a*), (*b*): the injected signal. Second row (*c*), (*d*): signal at the source location after recording and TR of the complete signal at the receivers. Third row (*e*), (*f*): after recording the full signal, but TR of only the u component. Fourth row (*g*), (*h*): after recording of only the p-pulse, but TR of the full p signal. Signals are normalized to one.

It is arguable which is better between the first and the third one. In fact, the first one better reproduces u, but has a larger v-component (which does not exist in the input signal). This might not be, however, too relevant, since mode conversion starts right at the onset of the injection and the v-component is very small in both cases.

Next we wish to demonstrate the capability of TRE to focus energy on a scatterer in a solid. For this purpose, we consider a plate discretized as a lattice of 400×400 grid elements with space step $\varepsilon = 3\,\mathrm{mm}$. The plate has a void inclusion of 20×20 steps (best viewed as a black rectangle in the bottom plot of figure 13). We inject a compressional wave from a transducer of small but finite width with a Gaussian profile of width 42 μs. In figure 11 we observe the propagating pulse, right after injection in the upper plot; with a well formed P-wave front and a trailing S-mode (including also mode-reconverted P, see arrow, just as in figure 8) in the middle plot; and just reaching and illuminating the inclusion in the bottom plot.

When the pulse reaches the inclusion, it is partially reflected back to the source and time-reversed by an array of 11 equally spaced receivers, located on the left-hand side (pulse-echo mode). The retransmitted wavefield is enhanced to compensate for the losses (mostly the energy transmitted beyond the inclusion). The 'rays' from the 11 receivers/transmitters can be well observed in the upper plot of figure 12. The bottom plot shows good focusing of the resulting wavefield on the target (greyscale normalized to the maximum amplitude). The process is then repeated one more time (figure 13) and a still better focalization can be observed on the bottom plot, thus demonstrating the focusing power of TRE iterations.

4. Conclusions

TRA and TRE waves represent a new research tool that has generated considerable excitement, both as an area of basic science and for its wealth of potential applications in several fields (many of which already successfully implemented). Not yet explored, but very promising, are applications to the Earth sciences. In all cases, virtual experiments, such as LISA simulations, may be very useful, if not to replace actual experiments, at least to help in performing them more efficiently and at a lower cost. To our knowledge this is the

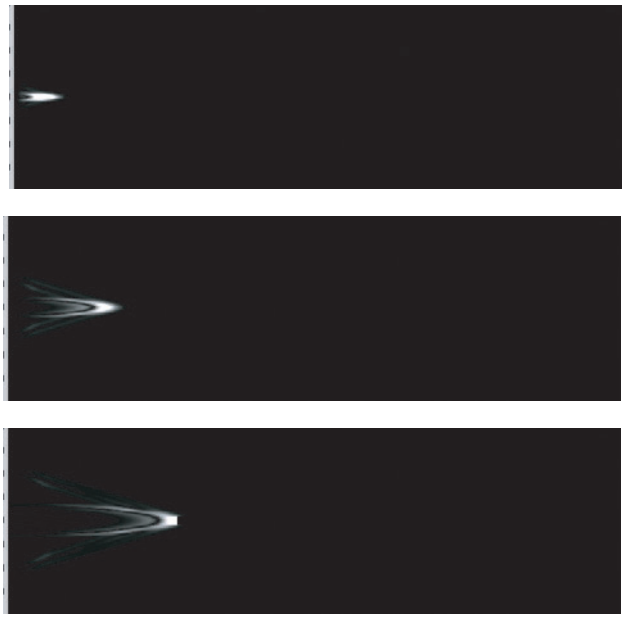

Figure 11. Propagation of a Gaussian pulse in an epoxy plate. The three plots represent three successive snapshots of the wavefield. Normalization as in figure 2; aspect ratio 1 : 3.

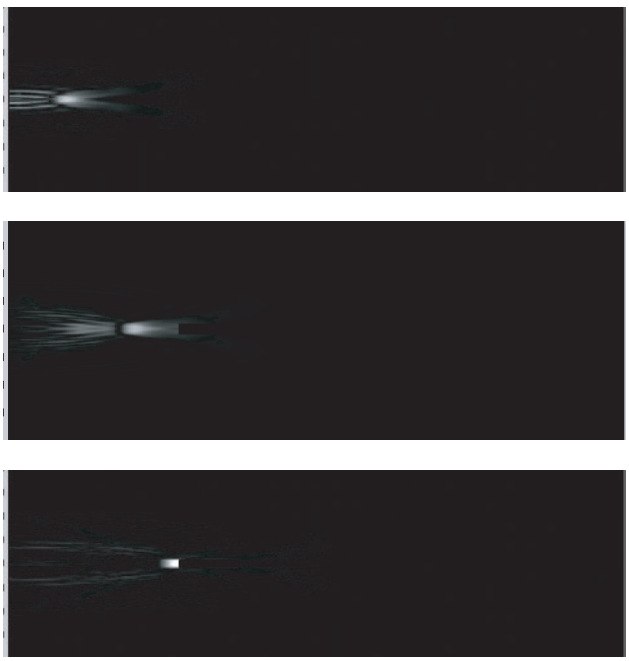

Figure 12. Wavefield due to the pulse of figure 11 after one TRE application. Normalization as in figure 2; aspect ratio 1 : 3.

first application of a simulation approach to elastic waves and opens up the possibility to apply our approach to more complex cases, such as anisotropic or stochastic media.

In the present contribution, we demonstrate the applicability of LISA to simulate both TRA and TRE experiments, by means of several examples. In particular, we illustrate the focusing power of both techniques, the advantage of multiple reflections (e.g. from the walls of a waveguide) and of multiple iterations. We also offer a preliminary comparative analysis of various different ways to include mode converted

Figure 13. Wavefield due to the pulse of figure 11 after two TRE applications. Normalization as in figure 2; aspect ratio 1 : 3.

pulses in the implementation of TRE. Finally, we demonstrate TRE's capability of focusing energy on a given target.

Acknowledgments

This work was partly supported by the INFM Parallel Computing Initiative (Italy). One of us (MS) wishes to thank the INFM for the financial support received in the framework of the 'Visiting Scientist INFM Parallel Computing Initiative'. The authors also acknowledge the support of the Institute for Geophysics and Planetary Physics and Institutional support (LDRD) at Los Alamos.

References

[1] Fink M *et al* 2000 *Rep. Prog. Phys.* **63** 1933
[2] Huang L-J, Fehler M and Wu R-S 1999 *Geophys.* **64** 1524
[3] Huang L-J, Fehler M, Roberts P and Burch C C 1999 *Geophysics* **64** 1535
[4] Huang L-J and Fehler M 2000 *Geoph. J. Int.* **140** 521
[5] Prada C *et al* 1996 *J. Acoust. Soc. Am.* **99** 2067
[6] Prada C and Fink M 1998 *J. Acoust. Soc. Am.* **104** 801
[7] Derode A, Roux P and Fink M 1995 *Phys. Rev. Lett.* **75** 4206
[8] Derode A, Tourin A and Fink M 1999 *J. Appl. Phys.* **85** 6343
[9] Roux P, Roman B and Fink M 1997 *Appl. Phys. Lett.* **70** 1811
[10] Fink M 1993 *J. Phys. D: Appl. Phys.* **26** 1333
[11] Fink M 1997 *Phys. Today* **50** 34
[12] Fink M 1999 *Scient. Am.* **281** 91
[13] Feuillade C and Clay C S 1992 *J. Acoust. Soc. Am.* **92** 2165
[14] Kupperman W A *et al* 1998 *J. Acoust. Soc. Am.* **103** 25
[15] Hodgkiss W *et al* 1999 *J. Acoust. Soc. Am.* **105** 1597
[16] Song H *et al* 1999 *J. Acoust. Soc. Am.* **105** 3176
[17] Hinkelman L M *et al* 1994 *J. Acoust. Soc. Am.* **95** 530
[18] Thomas J-L, Wu F and Fink M 1996 *Ultras. Imag.* **18** 106
[19] Delsanto P P *et al* 1992 *Wave Motion* **15** 65
Delsanto P P *et al* 1994 *Wave Motion* **20** 29

[20] Delsanto P P, Mignogna R, Scalerandi M and Schechter R 1998 Simulation of ultrasonic pulse propagation in complex media *New Perspectives on Problems in Classical and Quantum Physics* vol 2, ed P P Delsanto and A W Saenz (New Delhi: Gordon & Breach) pp 51–74
[21] Delsanto P P and Scalerandi M 1998 *J. Acoust. Soc. Am.* **104** 2584–91
[22] Schechter R S, Chaskelis H H, Mignogna R B and Delsanto P P 1994 *Science* **265** 1188
[23] Delsanto P P *et al* 1994 *Wave Motion* **26** 329
Scalerandi M and Agostini V 2002 *J. Comput. Ac.* **10** 275
[24] Scalerandi M *et al* 2002 *J. Ac. Soc. Am.* submitted
Scalerandi M *et al* 2002 *J. Phys. D: Appl. Phys.* submitted